

# Crystal Growth and X-ray Diffraction Characterization of Sb<sub>2</sub>Te<sub>3</sub> Single Crystal

Indu Rajput, Sumesh Rana, Rudra Prasad Jena and Archana Lakhani<sup>a</sup>

*UGC-DAE Consortium for Scientific Research, University Campus, Khandwa Road, Indore-452001, INDIA.*

<sup>a)</sup> Corresponding author: archnalakhani@gmail.com

**Abstract.** We report the single crystal growth and X-ray diffraction characterization of bulk Sb<sub>2</sub>Te<sub>3</sub> single crystal. Single crystal of Sb<sub>2</sub>Te<sub>3</sub> was grown by modified Bridgman method. The diffraction peaks corresponding to {0, 0, 3} planes reveal the growth of crystal along the c-direction. X-ray diffraction analysis by rietveld refinement confirms and verifies the phase purity, rhombohedral structure and single crystalline nature of the prepared Sb<sub>2</sub>Te<sub>3</sub> crystal. Unit cell structure of Sb<sub>2</sub>Te<sub>3</sub> consist of three quintuple layers stacked one above the other.

## INTRODUCTION

Discovery of topological insulators have drawn new interest in condensed matter physics because of their intriguing physical properties and novel device applications like spintronics, thermoelectric, and quantum computing [1–3]. Topological insulators possess bulk band gap like an ordinary band insulator but have topologically protected metallic surface states on their surface or edges [4–6]. The two factors responsible for these exotic surface states are spin-orbit interaction and time-reversal symmetry. The widely studied examples of topological insulators are Bi<sub>2</sub>Se<sub>3</sub>, Bi<sub>2</sub>Te<sub>3</sub> and Sb<sub>2</sub>Te<sub>3</sub> by various measurements. The fascinating physical properties in these topologically insulating materials like large magnetoresistance, weak antilocalization (WAL), high mobility makes them suitable for technical applications [7–9]. Most of the studies in literature on TIs are on thin films whereas the single crystals are comparatively less studied. The formation of single crystals of these TIs depends on the process followed during the preparation which highly determines the observed physical properties. For example the type of defects present in the Bi<sub>2</sub>Se<sub>3</sub> crystals gives rise to various interesting properties like large linear magnetoresistance,  $\pi$ -berry phase and the observation of quantum hall effect etc [10–13].

Sb<sub>2</sub>Te<sub>3</sub> is a well-known narrow-gap semiconductor with a band gap  $\sim 0.26$  eV which is demonstrated as a topological insulator experimentally by measurements like angle resolved photoemission spectroscopy (ARPES) [14]. Sb<sub>2</sub>Te<sub>3</sub> is a p-type topological insulator due to the holes which is introduced by Sb/Te antisite defects [15]. It would be interesting to study the structural correlation with physical properties like in magneto-transport properties due to the inherent characteristics and defects/in-homogeneities created during the crystal formation. With this aim we have prepared the single crystal of Sb<sub>2</sub>Te<sub>3</sub> and here we present its growth and structural characterization.

## EXPERIMENTAL DETAILS

Single crystal of Sb<sub>2</sub>Te<sub>3</sub> was grown by modified Bridgman method. The high purity elements of Sb (99.999%) and Te (99.999%) were accurately weighed in their stoichiometric ratio. The sample was melted at 850°C followed by cooling and annealing at about 600°C for a couple of days. As grown crystal of Sb<sub>2</sub>Te<sub>3</sub> was cleaved from which a smooth and shiny surface was found for structural characterization. X-ray diffraction of grown Sb<sub>2</sub>Te<sub>3</sub> single crystal was carried out using the Bruker D8 Advance x-ray diffractometer that used the Cu  $k_{\alpha}$  radiation having the wavelength 1.54Å.

## RESULTS AND DISCUSSION

Structural characterization of as grown  $\text{Sb}_2\text{Te}_3$  single crystal is carried out by X-ray diffraction measurement. **FIGURE 1** shows the powder XRD data along with its rietveld refinement. The x- axis indicates the  $2\theta$  values and y- axis represents the intensities corresponding to the  $2\theta$  values. The red circles are the observed data points and black lines show the fitted pattern obtained using Fullprof Suite software. The blue line indicates the difference between the experimental and theoretical fit. The complete overlap of the experimental and theoretical pattern obtained after the refinement and absence of any extra peaks in the calculated pattern confirms the single phase formation of the sample and its rhombohedral structure with R-3m (D5) space group. The green lines indicate the corresponding Bragg peaks.

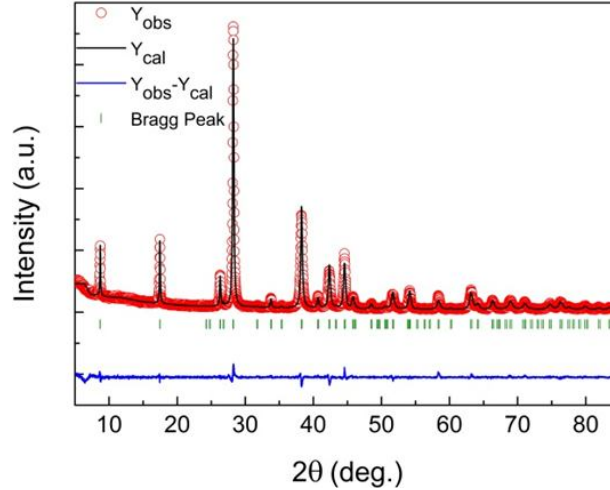


**FIGURE 1:** Room temperature powder X-ray diffraction data along with its Rietveld refinement fit.

The goodness of fit obtained from the refinement is 1.98 indicating the proper fit to the data. The fitting parameters obtained such as lattice constants,  $c/a$  ratio, volume etc. have been tabulated in **TABLE 1**. The lattice parameters obtained from the rietveld refinement are in well agreement with the earlier reports in the literature [16]. The obtained Wyckoff positions for our crystal are as follows; Sb position 6c (0,0,0.3992);  $\text{Te}^1$  position 3a (0,0,0);  $\text{Te}^2$  position 6c (0,0,0.2122). The approximate occupancy for Sb (6c) is 2.373,  $\text{Te}^1$ (3a) is 1.1975 and  $\text{Te}^2$ (6c) is 2.380. **FIGURE 2** shows the crystal structure of  $\text{Sb}_2\text{Te}_3$  generated using the VESTA software. The obtained unit cell structure of the grown  $\text{Sb}_2\text{Te}_3$  crystal exhibits the layered atomic arrangement in the rhombohedral structure which consists of three quintuple layers (QLs) and each quintuple layer contains five atoms in the order of ( $\text{Te}^1$ -Sb- $\text{Te}^2$ -Sb- $\text{Te}^1$ ). These superscripts (1) and (2) represent the distinctly bonded tellurium atoms. Adjacent quintuple layers are bonded with each other by weak vander Walls (vdW) forces and shows the presence of vander wall gap in between the two QLs, while atoms within the QLs are covalently bonded.

**TABLE 1:** Refined values of the parameters obtained from the Rietveld refinement

$a = b$ (Å)	$c$ (Å)	$c/a$	Volume(Å <sup>3</sup> )	$\chi^2$
4.264(3)	30.48(2)	7.143(2)	480.72(4)	1.98

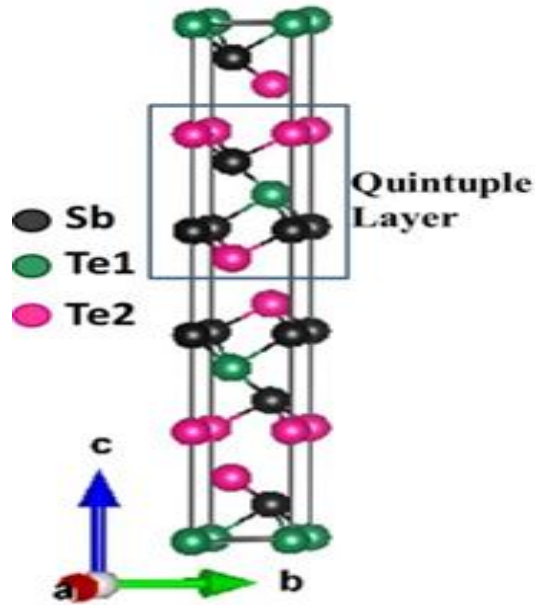


**FIGURE 2:** Crystal structure of  $\text{Sb}_2\text{Te}_3$  by VESTA software obtained by using parameters refined from rietveld refinement, showing quintuple layers.

Apart from powder X-ray diffraction of the obtained sample we performed the X-ray diffraction on the cleaved surface of the single crystal also the shiny flat surface is obtained after crystal cleaving. XRD pattern of cleaved surface of  $\text{Sb}_2\text{Te}_3$  crystal suggests that growth is along c- direction which as shown in **FIGURE 3**. All the diffraction peaks of the grown  $\text{Sb}_2\text{Te}_3$  single crystal were indexed with the help of standard JCPDS file for  $\text{Sb}_2\text{Te}_3$ . The large intensity of peaks corresponding to the  $\{003\}$  planes assures the single crystalline nature of the grown single crystal and the orientation of our crystal is along the c-axis.

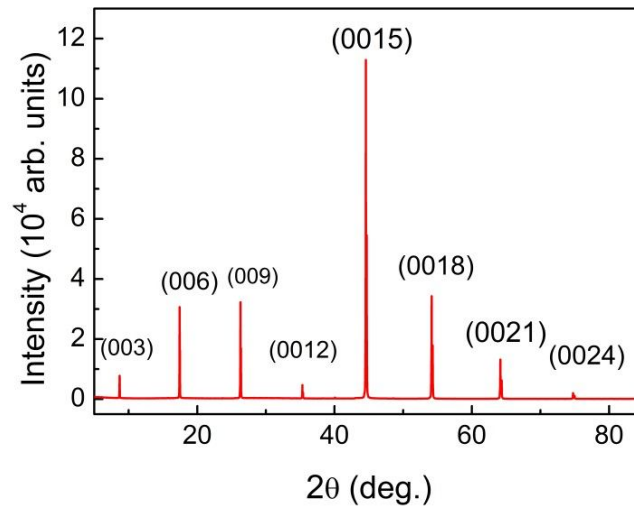


**FIGURE 3:** X-ray diffraction pattern for the cleaved crystal of  $\text{Sb}_2\text{Te}_3$ . The peaks corresponding to  $\{003\}$  planes indicate orientation of crystal planes along c-direction.

## CONCLUSION

A successful attempt to grow a single crystal of  $\text{Sb}_2\text{Te}_3$  by modified Bridgeman method was made. We confirm the single crystalline formation of  $\text{Sb}_2\text{Te}_3$  crystal, which is oriented along the c-axis. Rietveld refinement analysis confirmed the rhombohedral structure having (R-3m) space group and the occupancies of Sb,  $\text{Te}^1$ , and  $\text{Te}^2$  atoms. The formation of quintuple layers stacked over one another in the  $\text{Sb}_2\text{Te}_3$  crystal is visualized by using VESTA software. These layers are bound by vander Waals (vdW) forces having atom bonded by covalent bonds.

## ACKNOWLEDGMENTS

Authors thank Dr. M. Gupta and Er. L. Behera for XRD measurements, Dr. Devendra Kumar for useful discussion, Director Dr. A. K. Sinha and Centre Director Dr. V. Ganesan for encouragement and motivation.

## REFERENCES

1. I. Vobornik, U. Manju, J. Fujii, F. Borgatti, P. Torelli, D. Krizmancic, Y. S. Hor, R. J. Cava, and G. Panaccione, *Nano Lett.* **11**, 4079 (2011).
2. X. L. Qi and S. C. Zhang, *Rev. Mod. Phys.* **83**, (2011).
3. N. Xu, Y. Xu, and J. Zhu, *Npj Quantum Mater.* **1** (2017).
4. M. Z. Hasan and C. L. Kane, *Rev. Mod. Phys.* **82**, 3045 (2010).
5. H. Zhang, C.-X. Liu, X.-L. Qi, X. Dai, Z. Fang, and S.-C. Zhang, *Nat. Phys.* **5**, 438 (2009).
6. J. Moore, *Nat. Phys.* **5**, 378 (2009).
7. J. G. Checkelsky, J. Ye, Y. Onose, Y. Iwasa, and Y. Tokura, *Nat. Phys.* **8**, 729 (2012).
8. D. X. Qu, Y. S. Hor, J. Xiong, R. J. Cava, and N. P. Ong, *Science* (80)**329**, 821 (2010).
9. B. Hamdou, J. Gooth, A. Dorn, E. Pippel, and K. Nielsch, *Appl. Phys. Lett.* **102**, 1 (2013).
10. Devendra Kumar and Archana Lakhani, *Phys. Status Solidi RRL*, 1800088, 2018.
11. Devendra Kumar and Archana Lakhani, *Mater. Res. Bull.* **88**, 127 (2017).
12. Devendra Kumar and Archana Lakhani, *Phys. Status Solidi - Rapid Res. Lett.* **9**, 636 (2015).
13. A. Tayal, Devendra Kumar, and Archana Lakhani, *J. Phys. Condens. Matter* **29**, 445704 (2017).
14. D. Hsieh, Y. Xia, D. Qian, L. Wray, F. Meier, J. H. Dil, J. Osterwalder, L. Patthey, A. V. Fedorov, H. Lin, A. Bansil, D. Grauer, Y. S. Hor, R. J. Cava, and M. Z. Hasan, *Phys. Rev. Lett.* **103**, 2 (2009).
15. Z. Zhang, X. Feng, M. Guo, Y. Ou, J. Zhang, K. Li, L. Wang, X. Chen, Q. Xue, X. Ma, K. He, and Y. Wang, *Phys. Status Solidi RRL* **7**, No. 1-2, 142-144 (2013).
16. T. L. Anderson and H. B. Krause, *Acta Crystallogr* **30(5)**, 1307-1310 (1974).